

# Synthesis, Characterization and Catalytic Properties of Nanocrystalline $Y_2O_3$ -coated $TiO_2$ in the Ethanol Dehydration Reaction

Humberto Vieira Fajardo<sup>a\*</sup>, Elson Longo<sup>b</sup>, Edson Roberto Leite<sup>c</sup>, Rafael Libanori<sup>c</sup>,

Luiz Fernando Dias Probst<sup>d</sup>, Neftalí Lenin Villarreal Carreño<sup>e</sup>

<sup>a</sup>Departamento de Química, Universidade Federal de Ouro Preto – UFOP,  
CEP 35400-000, Ouro Preto, MG, Brasil

<sup>b</sup>Departamento de Físico-Química, Universidade Estadual Paulista – UNESP,  
CEP 14800-900, Araraquara, SP, Brasil

<sup>c</sup>Departamento de Química, Universidade Federal de São Carlos – UFSCar,  
CEP 13565-905, São Carlos, SP, Brasil

<sup>d</sup>Departamento de Química, Universidade Federal de Santa Catarina – UFSC,  
CEP 88040-900, Florianópolis, SC, Brasil

<sup>e</sup>Departamento de Química Analítica e Inorgânica, Universidade Federal de Pelotas – UFPel,  
CEP 96010-900, Capão do Leão, RS, Brasil

Received: August 18, 2011; Revised: January 23, 2012

In the present study,  $TiO_2$  nanopowder was partially coated with  $Y_2O_3$  precursors generated by a sol-gel modified route. The system of nanocoated particles formed an ultra thin structure on the  $TiO_2$  surfaces. The modified nanoparticles were characterized by high resolution transmission electron microscopy (HR-TEM), X-ray diffraction (XRD) analysis, Zeta potential and surface area through  $N_2$  physisorption measurements. Bioethanol dehydration was used as a probe reaction to investigate the modifications on the nanoparticles surface. The process led to the obtainment of nanoparticles with important surface characteristics and catalytic behavior in the bioethanol dehydration reaction, with improved activity and particular selectivity in comparison to their non-coated analogs. The ethylene production was disfavored and selectivity toward acetaldehyde, hydrogen and ethane increased over modified nanoparticles.

**Keywords:** *catalysis, surface modifications, titania, coating*

## 1. Introduction

Metal oxides are a subject of intense research in materials science. These oxides play an important role in heterogeneous catalysis, acting as active phase, promoter or support of solid catalysts. The catalytic properties of solids are highly dependent on their surface features. It is well known that the final structural characteristics of the catalysts are dependent on their preparation methods. In this sense, new synthesis methods, which lead to materials with superior performances, have been reported<sup>1-3</sup>. There is a general consensus that the possibility of preparing oxide particles on a nanoscale level would be very interesting due to its special physical and chemical properties in comparison to those of bulk particles<sup>4-7</sup>. The combination of two materials on a nanometer scale, one acting as the core and the other as the coating, can result in interesting surface modifications that are substantially different from those of the core, thus making the nanocoated particles attractive for several applications, including in catalysis<sup>8-10</sup>. The control of surfaces and the modifications of the structures of the particles can be used to obtain additional information on the catalytic properties and applications of these nanostructured materials.

Titanium oxide nanoparticles have been previously investigated by our group<sup>11-14</sup>. It is well known that this semiconducting oxide has excellent potential for several applications, due to its high capacity to adsorb gaseous molecules and to promote reactions over its surface<sup>4,11-14</sup>. The present paper focuses on the preparation and characterization of surface-modified  $TiO_2$  nanoparticles, using  $Y_2O_3$  as an insulating oxide, revealing its effects on their catalytic performances in the bioethanol dehydration reaction. Recently, a number of publications report experimental catalytic studies for the aforementioned reaction, discussing the utilization of different catalysts. From the data reported, not only the operational conditions employed, but also the nature of the catalyst used, has been shown to influence the catalytic performance. The ethanol dehydration process has gained increasing attention due to the possibility of obtaining ethylene, which is considered a valuable raw material in the petrochemical industry. Conventionally, ethylene is commercially produced by the thermal cracking of liquefied petroleum gas or naphtha processes, which require high temperatures. In contrast, catalytic dehydration of ethanol to ethylene requires lower temperatures and can offer higher ethylene yields<sup>15-19</sup>.

\*e-mail: hfajardo@iceb.ufop.br

## 2. Experimental Procedure

### 2.1. Sample preparation

The surface-modified  $\text{TiO}_2$  samples were obtained based on the sol-gel modified route, also known as in situ polymerizable complex method<sup>14,20</sup>. The starting materials were yttrium carbonate (Aldrich Co.), titanium oxide (P25; ca. 80% anatase and 20% rutile, Degussa Co.), citric acid (Mallinckrodt) and ethylene glycol (Mallinckrodt). Colloidal dispersions containing 2 g of commercial  $\text{TiO}_2$  nanoparticles in 50 mL of deionized water were prepared. The  $\text{TiO}_2$  powder was dispersed in water using an ultrasonic probe. An yttrium polymeric precursor water-based solution was used to coat the  $\text{TiO}_2$  nanoparticles. A polymeric resin was obtained by quelating a metal ion from the yttrium salt ( $\text{Y}_2(\text{CO}_3)_3$  – Aldrich Co.) with citric acid ( $\text{C}_6\text{H}_8\text{O}_7$  – Mallinckrodt), followed by polymerization against ethylene glycol ( $\text{C}_2\text{H}_4(\text{OH})_2$  – Mallinckrodt). The obtained resins were added into colloidal dispersions to obtain dispersions containing 0.4% ( $\text{TiO}_2\text{-Y}_2\text{O}_3(0.4)$ ); 0.8% ( $\text{TiO}_2\text{-Y}_2\text{O}_3(0.8)$ ); 1.2% ( $\text{TiO}_2\text{-Y}_2\text{O}_3(1.2)$ ); 2.4% ( $\text{TiO}_2\text{-Y}_2\text{O}_3(2.4)$ ) in weight of  $\text{Y}_2\text{O}_3$  per weight of  $\text{TiO}_2$ . These dispersions were sonicated for 10 minutes and the aqueous solvent was removed using a rotary evaporator. The resultant solid was pulverized and calcined, in an air atmosphere, at 450 °C for 4 hours. The complexation of yttrium with citric acid and the posterior esterification reaction between metal citrate and ethylene glycol is illustrated in Figure 1<sup>[21]</sup>.

### 2.2. Sample characterization

The structure and morphology of the samples were studied by high resolution transmission electron microscopy (HRTEM - Philips CM 200). The specific surface areas (B.E.T. method) of the samples were determined by  $\text{N}_2$  adsorption/desorption isotherms at liquid nitrogen temperature by means of an Autosorb-1C analyzer (Quantachrome Instruments). The zeta potential of the dilute suspensions was measured in a Zeta Potential Meter (Brookhaven Inst. Corp. Zetaplus). Phase identification was carried out by X-ray diffraction (XRD) analysis (D5000, Siemens, Germany) using  $\text{CuK}\alpha$  radiation.

### 2.3. Catalytic tests

Catalytic performance tests were conducted at atmospheric pressure with a quartz fixed-bed reactor (inner diameter 12 mm) fitted in a programmable oven, at 500 °C. The water:ethanol mixture, of known composition, was pumped into a heated chamber (kept at 200 °C) and vaporized. The water-ethanol gas ( $\text{N}_2$ ) stream (30 mL/min) was then fed to the reactor containing 100 mg of the catalyst powder. The reactants and the composition of the reactor effluent were analyzed on line with a gas chromatograph (Shimadzu GC 8A).

## 3. Results and Discussion

### 3.1. Characterization

The samples were characterized by HRTEM, after the annealing process, in order to understand the effect

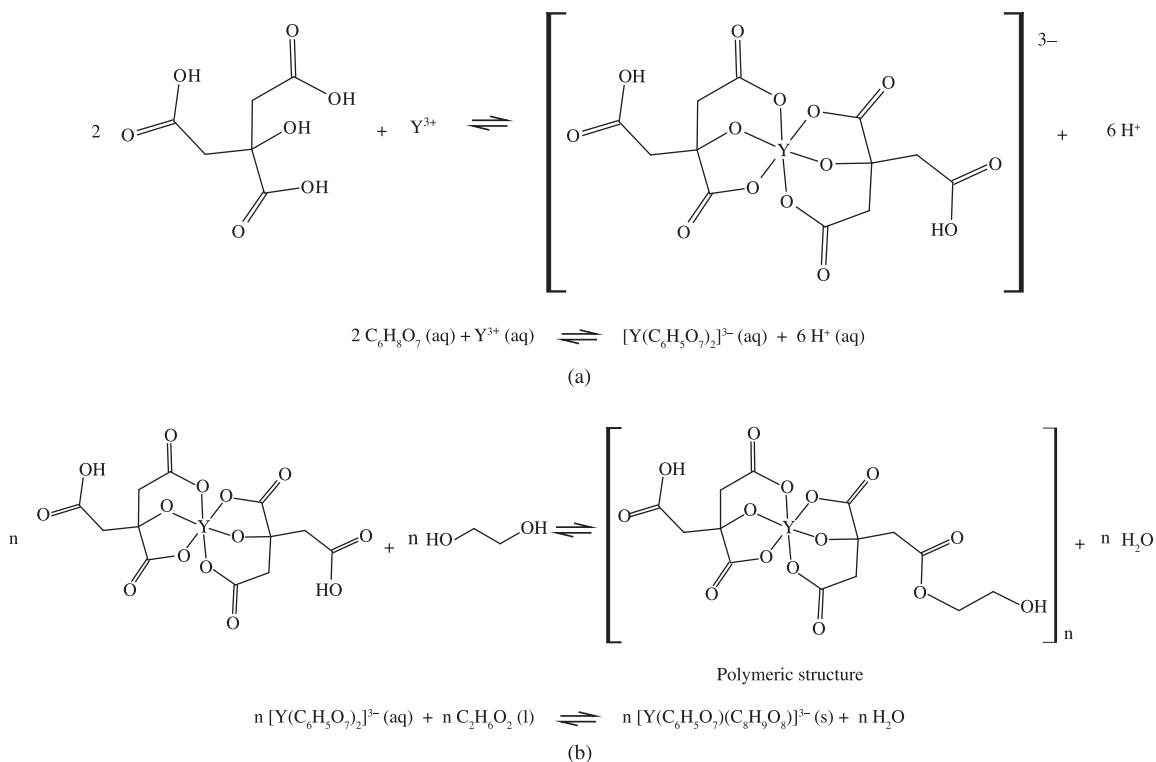


**Figure 1.** Schematic representation of the metal-citric acid complex and polymeric precursor formation.

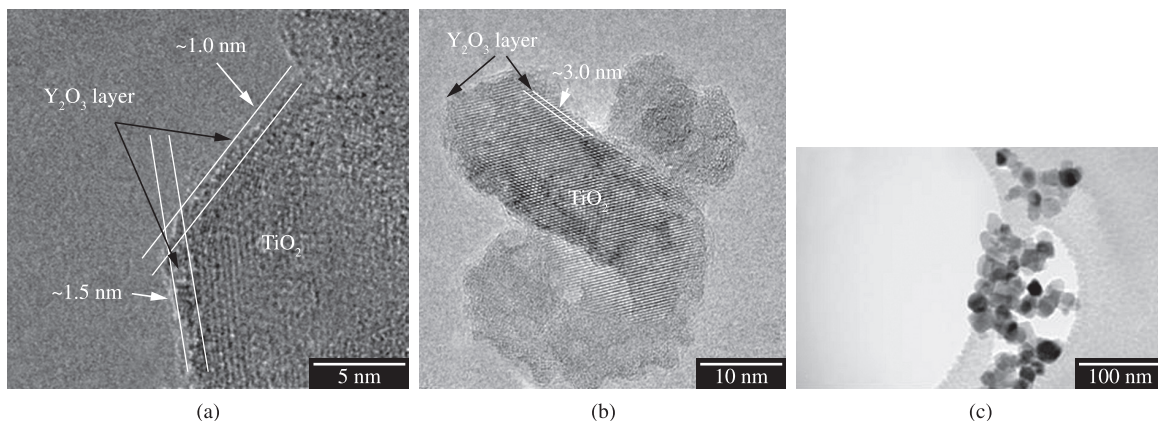


**Figure 2.** HRTEM images of  $\text{TiO}_2$  nanoparticles modified with  $\text{Y}_2\text{O}_3$ : a)  $\text{TiO}_2\text{-Y}_2\text{O}_3(0.4)$ ; b)  $\text{TiO}_2\text{-Y}_2\text{O}_3(0.8)$ ; and c) modified nanoparticles exhibiting a spherical morphology and similar size.

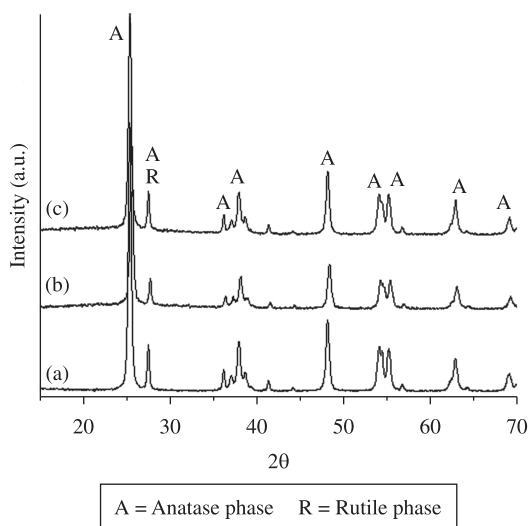


**Figure 3.** X-ray diffraction patterns for  $\text{Y}_2\text{O}_3$  coating of  $\text{TiO}_2$  nanopowders: a)  $\text{TiO}_2\text{-Y}_2\text{O}_3(0.4)$ ; b)  $\text{TiO}_2\text{-Y}_2\text{O}_3(1.2)$ ; and c)  $\text{TiO}_2\text{-Y}_2\text{O}_3(2.4)$ .

of nanocoating on the titania particle surface, which can be confirmed by the images of the partially coated  $\text{TiO}_2$ , shown in Figure 2. All the modified nanoparticles exhibit a spherical morphology and similar size, despite agglomerate formation (Figure 2c). Such images reveal the formation of irregular islands on the  $\text{TiO}_2$  surfaces, which consist of a crystalline core of  $\text{TiO}_2$  surrounded by an amorphous coating of ultra thin thickness of  $\text{Y}_2\text{O}_3$  (0.4 and 0.8% mass of  $\text{Y}_2\text{O}_3$ , shown in Figure 2a,b, respectively). The thickness of the thin coating layer on the  $\text{TiO}_2$  particles was related to the  $\text{Y}_2\text{O}_3$  concentration of the nanocoating. The thickness of the coating is at a range that goes from 1.0 to 3.0 nm. These observations are corroborated by the HRTEM analysis of the  $\text{TiO}_2\text{-Y}_2\text{O}_3$  samples. The crystal structure of the nanocomposites based on the nanocoating of the  $\text{Y}_2\text{O}_3$  additive on  $\text{TiO}_2$  and the respective XRD patterns are shown in Figure 3. In this pattern the peaks can be only ascribed to the tetragonal anatase phase of

**Table 1.** Physical-chemical characterizations of unmodified ( $\text{TiO}_2$ ) and modified ( $\text{TiO}_2\text{-Y}_2\text{O}_3$ ) nanoparticles.

Samples	$S_{(\text{B.E.T})}^a$ ( $\text{m}^2\cdot\text{g}^{-1}$ )	I.E. <sup>b</sup>
$\text{TiO}_2$	81	2.6
$\text{TiO}_2\text{-Y}_2\text{O}_3(0.4)$	51	–
$\text{TiO}_2\text{-Y}_2\text{O}_3(0.8)$	52	–
$\text{TiO}_2\text{-Y}_2\text{O}_3(1.2)$	51	–
$\text{TiO}_2\text{-Y}_2\text{O}_3(2.4)$	50	4.6

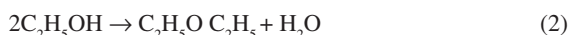
a = specific surface area, calculated according B.E.T. method. b = isoelectric point, obtained graphically by Zeta potential measurements, for the catalysts.

crystalline  $\text{TiO}_2$ , however, the reflection peak at  $2\theta = 27^\circ$  can also be assigned to rutile phase, indicating the mixture constitutes phases. No diffraction peaks related to the yttrium oxide phase were observed in the nanocoated  $\text{TiO}_2$  samples, respectively. A similar finding has been previously reported by Gonçalves et al.<sup>22</sup> for  $\text{ZrO}_2$  powder coated with low concentrations of  $\text{Al}_2\text{O}_3$ . Additional information on the textural properties, specific surface area values, of the partially nanocoated  $\text{TiO}_2$  samples is summarized in Table 1. The pure  $\text{TiO}_2$  sample presented the highest specific surface area,  $81 \text{ m}^2\cdot\text{g}^{-1}$ . For the surface-modified samples, specific surface area values were very similar. The comparison shows that the heat treatment employed in the surface modification process resulted in a similar surface area decrease, approximately 37% for all modified nanoparticles, when compared with unmodified nanoparticles. The isoelectric values (graphically obtained by Zeta potential measurements) are compiled in Table 1. We can see that the addition of different amounts of insulating yttrium oxide on the  $\text{TiO}_2$  nanoparticles gave different isoelectric point values, indicating that the surface chemical composition changed and an increase of  $\text{Y}_2\text{O}_3$  concentration on the surface may be assumed<sup>14</sup>.

### 3.2. Catalytic performances

In order to investigate the catalytic behavior of the samples, the ethanol dehydration reaction was carried out.

In addition, this process could be used as a probe reaction to evaluate the modifications on the nanoparticles surface. During catalytic dehydration of ethanol, intramolecular dehydration of ethanol to ethylene (Equation 1) and intermolecular dehydration to diethyl-ether (Equation 2) can occur in parallel. At lower temperatures, diethyl-ether is produced in significant quantities, while at higher temperatures ethylene is the major product<sup>16</sup>.



It was observed, from the product distribution shown in Figure 4, that the steam reforming reaction of ethanol (Equation 3) over the catalysts was negligible under the operational conditions employed. This is possibly due to the presence of water in the feed<sup>23</sup>.



However, it can be seen that hydrogen, ethylene and acetaldehyde were the only products detected during the process over the unmodified  $\text{TiO}_2$  catalyst (Figure 4a). Dehydration of ethanol, which occurs to an appreciable extent producing ethylene, seems to occur as the main reaction. A slight amount of acetaldehyde was also detected, at the beginning of the test, indicating that ethanol dehydrogenation to acetaldehyde (Equation 4) was promoted. However, during the last 150 minutes, dehydration of ethanol became the predominant reaction. According Zhang et al.<sup>16</sup> ethanol dehydrogenation to produce acetaldehyde can also occur as a side reaction at higher reaction temperatures.



The ethanol conversion decreased from 43 to 10% after 250 minutes on stream with a significant difference in the product distribution. The coke formation from ethylene polymerization (Equation 5) may be considered as the main reason for the catalyst deactivation observed in this case. The carbon deposited after the catalytic test was visually detected but not measured and characterized in this work.



In spite of the relatively low specific surface area presented, the  $\text{TiO}_2\text{-Y}_2\text{O}_3(2.4)$  catalyst achieved significant ethanol conversion values. A layer of yttrium oxide coating can increase the amount of adsorbing centers on the particle surface, which can improve and provide more active sites for further reactions. The modified catalyst presented a distinct behavior (Figure 4b), displaying a higher degree of selectivity toward  $\text{CH}_3\text{CHO}$  and  $\text{H}_2$  with lower formation of  $\text{C}_2\text{H}_4$ , indicating that the dehydrogenation reaction of ethanol was favored. Thus, a combination of catalytic properties could be observed on the surface, indicating that this particular catalyst has the ability for dehydration of ethanol and also some capacity for dehydrogenation of ethanol. The incorporation of  $\text{Y}_2\text{O}_3$ , an oxide with alkaline characteristics, into the  $\text{TiO}_2$  led to an increase in the acetaldehyde selectivity, favoring the dehydrogenation of ethanol. It is well known that the basic and acidic properties of the oxide catalysts are essential parameters directly affecting the primary selectivity for acetaldehyde or ethylene. Basic sites are predominant in the ethanol dehydrogenation to acetaldehyde, whereas ethylene would be produced with an essential role of the acidic sites of the oxides<sup>23</sup>. Therefore, a basic oxide, such as yttrium oxide, introduced in the  $\text{TiO}_2$  matrix promotes the basicity of the surface. The lower ethylene selectivity observed over the modified catalyst corroborates this fact. The surface modifications, due to coating process, change some properties of the titanium oxide, such as the

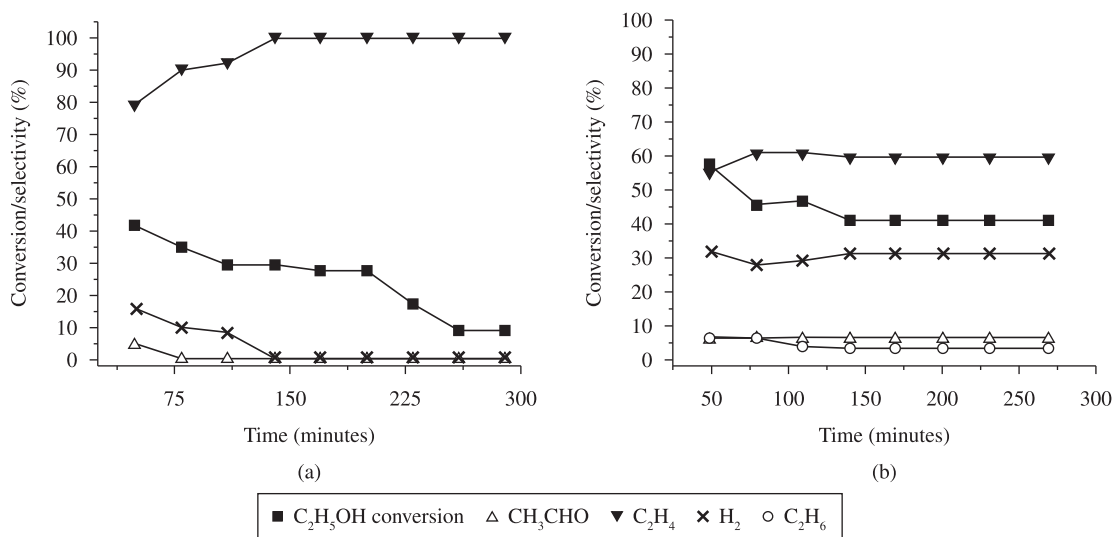


**Figure 4.** Catalytic performances in the dehydration of ethanol over: a)  $\text{TiO}_2$  pure sample; and b)  $\text{Y}_2\text{O}_3$  coated  $\text{TiO}_2$  ( $\text{TiO}_2\text{-Y}_2\text{O}_3(2.4)$ ).

isoelectric point. The isoelectric point of pure TiO<sub>2</sub> can be shifted to basic pH values via the introduction of a basic surface oxide (Y<sub>2</sub>O<sub>3</sub>). Thus, the basic characteristics of the rare earth oxide may favor some catalytic aspects such as the increase in the basicity of the surface<sup>24,25</sup>. In the present study, the quantitative determination of basic and acidic sites and its influence on the catalytic behavior was not reported. However, this study is under way and it will be subject of a future report. Even so, the occurrence of an ethanol decomposition reaction (Equation 6) can not be ruled out due to the high hydrogen selectivity value observed.



The conversion of ethanol using the TiO<sub>2</sub>-Y<sub>2</sub>O<sub>3</sub>(2.4) catalyst was higher than for the TiO<sub>2</sub> catalyst, and this catalyst kept a satisfactory ethanol conversion level until the end of the test, indicating the positive effect of Y<sub>2</sub>O<sub>3</sub> incorporation, in spite of the lower specific surface area of this sample compared to the pure TiO<sub>2</sub>. The very low concentration of ethane detected at the beginning of the test can be ascribed to the occurrence of ethylene hydrogenation (Equation 7)<sup>26</sup>. These observations are indicative of a moderate modification of the material surface due to the Y<sub>2</sub>O<sub>3</sub> incorporation.



## References

- Kung HH and Ko EI. Preparation of oxide catalysts and catalyst supports – a review of recent advances. *The Chemical Engineering Journal and the Biochemical Engineering Journal*. 1996; 64:203-214. [http://dx.doi.org/10.1016/S0923-0467\(96\)03139-9](http://dx.doi.org/10.1016/S0923-0467(96)03139-9)
- Campanati M, Fornasari G and Vaccari A. Fundamentals in the preparation of heterogeneous catalysts. *Catalysis Today*. 2003; 77:299-314. [http://dx.doi.org/10.1016/S0920-5861\(02\)00375-9](http://dx.doi.org/10.1016/S0920-5861(02)00375-9)
- Schmidt F. New catalyst preparation technologies – observed from an industrial viewpoint. *Applied Catalysis A: General*. 2001; 221:15-21. [http://dx.doi.org/10.1016/S0926-860X\(01\)00802-X](http://dx.doi.org/10.1016/S0926-860X(01)00802-X)
- Fernández-García M, Martínez-Arias A, Hanson JC and Rodríguez JA. Nanostructured oxides in chemistry: characterization and properties. *Chemical Reviews*. 2004; 104:4063-4104. PMID:15352786. <http://dx.doi.org/10.1021/cr030032f>
- Caruso F, Caruso RA and Möhwald H. Nanoengineering of inorganic and hybrid hollow spheres by colloidal templating. *Science*. 1998; 282:1111-1114. PMID:9804547. <http://dx.doi.org/10.1126/science.282.5391.1111>
- Dierstein A, Natter H, Meyer F, Stephan HO, Kropf C and Hempelmann R. Electrochemical deposition under oxidizing conditions (EDOC): a new synthesis for nanocrystalline metal oxides. *Scripta Materialia*. 2001; 44:2209-2212. [http://dx.doi.org/10.1016/S1359-6462\(01\)00906-X](http://dx.doi.org/10.1016/S1359-6462(01)00906-X)
- Deki S, Yanagimoto H, Hiraoka S, Akamatsu K and Gotoh K. NH<sub>2</sub>-Terminated Poly(ethylene oxide) containing nanosized NiO particles: synthesis, characterization, and structural considerations. *Chemistry of Materials*. 2003; 15:4916-4922. <http://dx.doi.org/10.1021/cm021754a>
- Cendrowski K, Chen X, Zielinska B, Kalenczuk RJ, Rummeli MH, Büchner B et al. Synthesis, characterization, and photocatalytic properties of core/shell mesoporous silica nanospheres supporting nanocrystalline titania. *Journal of Nanoparticle Research*. 2011; 13:5899-5908. <http://dx.doi.org/10.1007/s11051-011-0307-1>
- Rosa ILV, Oliveira LH, Longo E and Varela JA. Synthesis and photoluminescence behavior of the Eu<sup>3+</sup> ions as a nanocoating over a silica Stöber matrix. *Journal of Fluorescence*. 2011; 21:975-981. PMID:20455013. <http://dx.doi.org/10.1007/s10895-010-0671-8>
- Kang KM, Kim HW, Shim IW and Kwak HY. Catalytic test of supported Ni catalysts with core/shell structure for dry reforming of methane. *Fuel Processing Technology*. 2011; 92:1236-1243. <http://dx.doi.org/10.1016/j.fuproc.2011.02.007>
- Leite ER, Carreño NLV, Santos LPS, Rangel JH, Soledade LEB, Longo E et al. Photoluminescence in amorphous TiO<sub>2</sub>-PbO system. *Applied Physics A*. 2001; 73:567-569. <http://dx.doi.org/10.1007/s003390100865>
- Ribeiro C, Longo E and Leite ER. Tailoring of heterostructures in a SnO<sub>2</sub>/TiO<sub>2</sub> system by the oriented attachment mechanism. *Applied Physics Letters*. 2007; 91:103-105. <http://dx.doi.org/10.1063/1.2779932>
- Carreño NLV, Garcia ITS, Carreño LSSM, Nunes MR, Leite ER, Fajardo HV et al. Synthesis of titania/carbon nanocomposites by polymeric precursor method. *Journal of Physics and Chemistry of Solids*. 2008; 69:1897-1904. <http://dx.doi.org/10.1016/j.jpcs.2008.01.014>

## 4. Conclusion

In this work, we obtained surface-modified TiO<sub>2</sub> nanoparticles, using Y<sub>2</sub>O<sub>3</sub> as an insulating oxide, by a sol-gel modified route. The observed structures showed that the proposed method is effective to the modification of TiO<sub>2</sub> surface, despite the irregular distribution of the insulating oxide. These surface modifications changed some properties of the powder, such as the isoelectric point, specific surface area and catalytic activity that were monitored through catalytic tests in ethanol dehydration reaction. It was found that the pure catalyst (TiO<sub>2</sub>) were very selective toward ethylene, which is a valuable raw material in the petrochemical industry. On the other hand, the modified catalyst TiO<sub>2</sub>-Y<sub>2</sub>O<sub>3</sub>(2.4) presented an improved activity and particular selectivity in comparison to their non-coated analogs. The ethylene production was disfavored and selectivity toward acetaldehyde, hydrogen and ethane increased over modified nanoparticles. This behavior may be related to the modification of the surface chemical composition due to the coating process.

## Acknowledgements

The authors wish to thank CNPq, FAPEMIG and FAPESP. Authors are in debt with Dr Jason Guy Taylor (DEQUI – UFOP) for insightful discussion and for reviewing the manuscript for its English usage.

14. Libanori R, Giraldo TR, Longo E, Leite ER and Ribeiro C. Effect of TiO<sub>2</sub> surface modification in Rhodamine B photodegradation. *Journal of Sol-Gel Science and Technology*. 2009; 49:95-100. <http://dx.doi.org/10.1007/s10971-008-1821-1>
15. Chen G, Li S, Jiao F and Yuan Q. Catalytic dehydration of bioethanol to ethylene over TiO<sub>2</sub>/γ-Al<sub>2</sub>O<sub>3</sub> catalysts in microchannel reactors. *Catalysis Today*. 2007; 125:111-119. <http://dx.doi.org/10.1016/j.cattod.2007.01.071>
16. Zhang X, Wang R, Yang X and Zhang F. Comparison of four catalysts in the catalytic dehydration of ethanol to ethylene. *Microporous and Mesoporous Materials*. 2008; 116:210-215. <http://dx.doi.org/10.1016/j.micromeso.2008.04.004>
17. Wu LP, Li XJ, Yuan ZH and Chen Y. The fabrication of TiO<sub>2</sub>-supported zeolite with core/shell heterostructure for ethanol dehydration to ethylene. *Catalysis Communications*. 2009; 11:67-70. <http://dx.doi.org/10.1016/j.catcom.2009.08.013>
18. Takahara I, Saito M, Inaba M and Murata K. Dehydration of ethanol into ethylene over solid acid catalysts. *Catalysis Letters*. 2005; 105:249-252. <http://dx.doi.org/10.1007/s10562-005-8698-1>
19. Zaki T. Catalytic dehydration of ethanol using transition metal oxide catalysts. *Journal of Colloid and Interface Science*. 2005; 284:606-613. PMID:15780300. <http://dx.doi.org/10.1016/j.jcis.2004.10.048>
20. Maciel AP, Leite ER, Longo E and Varela JA. Método sol-gel modificado para obtenção de alumina nanoencapsulada com terras raras. *Cerâmica*. 2005; 51:52-57. <http://dx.doi.org/10.1590/S0366-69132005000100010>
21. Carreño NLV, Leite ER, Santos LPS, Lisboa-Filho PN, Longo E, Araújo GCL, et al. Síntese, caracterização e estudo das propriedades catalíticas e magnéticas de nanopartículas de Ni dispersas em matriz mesoporosa de SiO<sub>2</sub>. *Química Nova*. 2002; 25:935-942.
22. Gonçalves RF, Godinho MJ, Leite ER, Maciel AP, Longo E and Varela JA. Nanocoating of Al<sub>2</sub>O<sub>3</sub> additive on ZrO<sub>2</sub> powder and its effect on the sintering behaviour in ZrO<sub>2</sub> ceramic. *Journal of Materials Science*. 2007; 42:2222-2225. <http://dx.doi.org/10.1007/s10853-006-1021-8>
23. Haryanto A, Fernando S, Murali N and Adhikari S. Current status of hydrogen production techniques by steam reforming of ethanol: a review. *Energy Fuels*. 2005; 19:2098-2106. <http://dx.doi.org/10.1021/ef0500538>
24. Fajardo HV, Longo E, Probst LFD, Valentini A, Carreño NLV, Nunes MR et al. Influence of rare earth doping on the structural and catalytic properties of nanostructured tin oxide. *Nanoscale Research Letters*. 2008; 3:194-199. PMID:3244857. <http://dx.doi.org/10.1007/s11671-008-9135-3>
25. Pereira GJ, Castro RHR, Hidalgo P and Gouvêa D. Surface segregation of additives on SnO<sub>2</sub> based powders and their relationship with macroscopic properties. *Applied Surface Science*. 2002; 195:277-283. [http://dx.doi.org/10.1016/S0169-4332\(02\)00567-6](http://dx.doi.org/10.1016/S0169-4332(02)00567-6)
26. Laosiripojana N and Assabumrungrat S. Catalytic steam reforming of ethanol over high surface area CeO<sub>2</sub>: The role of CeO<sub>2</sub> as an internal pre-reforming catalyst. *Applied Catalysis B: Environmental*. 2006; 66:29-39. <http://dx.doi.org/10.1016/j.apcatb.2006.01.011>